

Neutron Halo Structure Probed by Breakup Reactions

Takashi Nakamura

Department of Physics, Tokyo Institute of Technology, 2-12-1 O-Okayama, Meguro, Tokyo 152-8551

E-mail: nakamura@phys.titech.ac.jp

Abstract. The neutron drip line represents the boundary of nuclei in the neutron-rich side of the nuclear chart. In the vicinity of the neutron drip line, we often observe 'neutron halo' structure. We discuss how the neutron halo nuclei are studied by the breakup reactions at relativistic energies. Coulomb breakup is the dominant process in the breakup with a heavy target, such as Pb. In the Coulomb breakup of halo nuclei, enhancement of the electric dipole strength at low excitation energies (soft $E1$ excitation) is observed as a unique property for halo nuclei. The mechanism of the soft $E1$ excitation and its spectroscopic significance is shown as well as the applications of the Coulomb breakup to the very neutron rich ^{22}C and ^{31}Ne , which was measured at 230-240 MeV/nucleon at the new-generation RI beam facility, RIBF (RI Beam Factory), at RIKEN. Evidence of halo structures for these nuclei is provided as enhancement of the inclusive Coulomb breakup, which is a useful tool for the low-intense secondary beam. We also show that the breakup with a light target (C target), where nuclear breakup is a dominant process, can be used to extract the spectroscopic information of the removed neutron. The combinatorial analysis was found very useful to extract more-detailed information such as the spectroscopic factor and the separation energy. Prospects of the breakup reactions on neutron-drip line nuclei at RIBF at RIKEN are also briefly presented.

1. Introduction

Nuclear properties vary significantly from the β stability valley to the drip lines through the nuclear chart. Concerning the evolution of nuclear properties towards the neutron drip line, we address here the following questions: 1) Where is the neutron drip line?; 2) What are the characteristic features of drip-line nuclei?; and 3) How does nuclear structure evolve towards the neutron drip line?

About the first issue, the location of the neutron drip line has been established experimentally only up to $Z=8$ oxygen isotopes. By adding only one proton to the most neutron-rich oxygen isotope ^{24}O , the neutron drip line extends at least 6 neutrons farther, ^{31}F , and yet we do not know experimentally if this nucleus is on the drip line[1]. The location of the drip line offers a rigorous test of the structure and stability at the neutron-rich extreme, and as such, is one of the key issues of nuclear physics.

Concerning the second issue, one of the characteristic features of neutron drip line nuclei is halo structure, which has been found in the light neutron-rich nuclei. For almost a decade, the heaviest neutron halo nucleus known had been ^{19}C until evidence for the halo structure in ^{22}C and ^{31}Ne by breakup reactions was provided, which is discussed in this paper. For ^{22}C , an independent reaction measurement has indicated its two-neutron halo structure as well [2].

The shell evolution has drawn much attention concerning the third question. The island of inversion near $N=20$ neutron-rich nuclei is one of such examples. We note that shape evolution as well as halo formation towards the neutron drip line are also interesting issues. The shell evolution itself is often associated with deformation. Halo structure appears when the valence neutron of a nucleus has low or null orbital angular momentum. It is interesting to note that the shell modification often occurs for halo nuclei. In a sense, the evolution of shell, deformation, and halo formation are all closely related to each other. In the later section, we discuss how the ^{31}Ne nucleus has a halo structure, which is closely related to the shell evolution.

The neutron drip-line nuclei are special in the following reasons. When the Fermi levels between the neutrons and protons become very asymmetric in the neutron-rich side, the valence neutron becomes more and more weakly bound until it reaches the neutron drip line. Neutron halo can be formed in such a situation, which is helped by the fact that the valence neutron(s) are not affected by the Coulomb barrier. We also note that the excitation and coupling to the continuum become more significant. Because of these features, breakup reactions associated with $1n/2n$ emission play major roles in the spectroscopic studies of neutron halo nuclei.

One-neutron halo, such as in ^{11}Be and ^{19}C , is formed on the following conditions. Firstly, the separation energy should be small, typically less than 1 MeV. Another important requirement is that the valence neutron has low (or no) orbital angular momentum to avoid the hindrance of the tunneling effect due to the centrifugal barrier ($\ell(\ell+1)\hbar^2/(2\mu r^2)$). It is suggested that the orbital angular momentum should be $\ell=0$ or 1 for halo formation. In fact, only when $\ell=0, 1$ can one obtain a divergent r.m.s. radius ($\sqrt{\langle r^2 \rangle}$) of the extended neutron density distribution in the limit that $S_n \rightarrow 0$ [3].

For the two-neutron halo nuclei, such as ^{11}Li , we find further interesting features. A two neutron halo nucleus has Borromean three-body structure, where the involving two-body systems are all unbound, while this nucleus is barely bound as a three-body system. The dineutron correlation, a strong spatial nn correlation on the nuclear surface, has been studied intensively by theories [4, 5, 6], which could be explored in the breakup reactions as well.

2. Coulomb breakup and soft $E1$ excitation of halo nuclei

Coulomb breakup is a process, where a projectile passes by a high- Z target at relativistic energies, is excited, and decays in-flight into the charged fragment and nucleon(s). For instance for the classical halo nucleus ^{11}Be , the ^{11}Be projectile is excited by absorbing an $E1$ virtual photon, and decays into ^{10}Be and a neutron. When we measure the momentum vectors of both ^{10}Be and a neutron in coincidence, then the invariant mass of the intermediate excited state of ^{11}Be can be reconstructed. This is called a kinematical complete measurement or exclusive measurement. By using the equivalent photon prescription, energy differential Coulomb breakup cross section can be described as in,

$$\frac{d\sigma(E1)}{dE_x} = \frac{16\pi^3}{9\hbar c} N_{E1}(E_x) \frac{dB(E1)}{dE_x}, \quad (1)$$

where $N_{E1}(E_x)$ is the number of $E1$ virtual photons with photon energy E_x . With this measurement and the prescription, one can map $B(E1)$ as a function of E_x , or equivalently, $E_{\text{rel}} (= E_x - S_n)$.

One of the unique properties of halo nucleus is enhanced Coulomb breakup cross section, which can be attributed to the large low-lying electric dipole transitions (soft $E1$ excitation). This is unique since $E1$ excitation is usually exhausted almost fully by the Giant Dipole Resonance (GDR) at higher energies. In what follows in this section, the characteristic features of soft $E1$ excitation for $1n$ halo nuclei and $2n$ halo nuclei are briefly reviewed.

2.1. Soft $E1$ excitation of $1n$ halo nuclei

For a one-neutron halo nucleus, the soft $E1$ excitation has been explained as occurrence of direct breakup, where the halo nucleus breaks up into a core fragment and a neutron without forming a resonance. The final state is just a scattering continuum state. The matrix element of the direct breakup mechanism can be described as,

$$\frac{dB(E1)}{dE_{\text{rel}}} = |\langle \Phi_f(\vec{r}, \vec{q}) | e_{\text{eff}}^{E1} \hat{T}(E1) | \Phi_i(\vec{r}) \rangle|^2, \quad (2)$$

where $\Phi_i(\vec{r})$ and $\Phi_f(\vec{r}, \vec{q})$ represent the wave function of the ground state and the final state in the continuum of the neutron relative to the core, respectively. \vec{r} is the relative coordinate of the valence neutron relative to the c.m. of the core. $\Phi_f(\vec{r}, \vec{q})$ is also a function of the relative momentum $q = \sqrt{2\mu E_{\text{rel}}/\hbar}$. $\hat{T}(E1) (= rY^{(1)}(\Omega))$ represents the electric dipole operator.

For ^{11}Be , Φ_i is $|^{11}\text{Be}(1/2^+; \text{g.s.})\rangle$, which is described as,

$$|^{11}\text{Be}(1/2^+; \text{gs})\rangle = \alpha |^{10}\text{Be}(0^+) \otimes 2s_{1/2}\rangle + \beta |^{10}\text{Be}(2^+) \otimes 1d_{5/2}\rangle + \dots, \quad (3)$$

where the first term represents the halo configuration containing the s -wave neutron. Eq. (2) shows that the $B(E1)$ distribution has the form of Fourier transform of the ground state radial wave function, multiplied by the relative distance r between the core and the valence neutron. Hence, appearance of the extended radial distribution (halo configuration) leads to the large $B(E1)$ at very low relative energies, which is the mechanism of the soft $E1$ excitation for the one-neutron halo nucleus. For ^{11}Be , this happens for the first term in Eq. (3).

The important application of the soft $E1$ excitation of the one-neutron halo nucleus is that the $B(E1)$ distribution is only sensitive to the halo configuration. For ^{11}Be , only the first term contributes to the low-lying $E1$ strength. In turn, the shape and amplitude of the $B(E1)$ spectrum can be used to extract the spectroscopic information. For ^{11}Be , the amplitude is directly used to determine the amplitude of the first term in Eq. (3). In fact, the experiments determined $C^2S (= \alpha^2)$ of the halo configuration to be about 0.7 [7, 8, 9]. In the Coulomb breakup measurement of ^{19}C [10], the orbital angular momentum ℓ of the valence neutron, J^π of the ground state, and even the one-neutron separation energy, S_n , were extracted.

2.2. Soft $E1$ excitation of $2n$ halo nuclei

For $2n$ halo nuclei, such as ^{11}Li , due to the three-body nature, the $B(E1)$ strength distribution becomes more complex, compared to that for $1n$ halo nuclei. The $B(E1)$ strength of ^{11}Li , observed recently with high statistics [11], shows a peak at lower E_{rel} with larger amplitude, compared with the case of ^{11}Be . This is partially due to the effect of the spatial nn correlation (dineutron correlation). This can be seen by the non-energy weighted cluster sum rule, which can be described as,

$$B(E1) = \frac{3}{4\pi} \left(\frac{Ze}{A} \right)^2 \langle r_1^2 + r_2^2 + 2\vec{r}_1 \cdot \vec{r}_2 \rangle = \frac{3}{\pi} \left(\frac{Ze}{A} \right)^2 \langle r_{c,2n}^2 \rangle. \quad (4)$$

Here, \vec{r}_1 and \vec{r}_2 are the position vectors of the valence neutrons relative to the c.m. of the core. $r_{c,2n}$ is the distance between the c.m. of the core and that of the two halo neutrons. Importantly, the term of $\langle \vec{r}_1 \cdot \vec{r}_2 \rangle$ involves the opening angle $\langle \theta_{12} \rangle$ between \vec{r}_1 and \vec{r}_2 . The value of $\langle r_{c,2n} \rangle$, and hence $B(E1)$, becomes larger for the smaller spatial separation of the two neutrons as θ_{12} approaches 0° . The integrated $B(E1)$ thus provides a good measure of the two-neutron spatial correlation (dineutron correlation). The soft $E1$ excitation of two-neutron halo nuclei is thus important to probe the dineutron correlation.

3. Nuclear breakup and momentum distribution of the fragment

Nuclear Breakup with a light target is another powerful probe of exotic nuclei. In particular, the one neutron removal reaction has been used to extract the single particle property of the valence nucleon. Identification of the final core state, usually done by identifying the de-excitation γ ray, is used to extract the shell configuration, involving the ℓ value of the valence nucleon and its associated core state with the C^2S value.

The final core state could be unbound when the separation energy is small as in the vicinity of the neutron drip line. We have recently performed a measurement of the $1n$ removal reaction of the drip-line nucleus ^{14}Be with a proton target at about 69 MeV/nucleon [12]. The ^{13}Be residue is produced, which then decays into ^{12}Be and a neutron. The final state can be extracted by the invariant mass method, where we measure momentum vectors of ^{12}Be and the neutron in coincidence. The other useful observable is the momentum of the $^{12}\text{Be}+n$ in the rest frame of the ^{14}Be projectile, which has the information of the neutron removed. In this case, we extracted the transverse momentum distribution, which has a characteristic shape according to the ℓ value of the neutron removed in the first step.

In this experiment we have found that the first peak of the E_{rel} spectrum, corresponding to the ground state of ^{13}Be , is well characterized by the p -wave neutron. Namely, it was found that the ground state of ^{13}Be is an intruder $1/2^-$ state. The intruder ground state may be due to the strong deformation of this nucleus.

4. Inclusive breakup of ^{22}C and ^{31}Ne

The new-generation RI-Beam facility, RIBF (RI-Beam Factory) at RIKEN has been commissioned recently, and has enhanced the capabilities of drip-line physics due to its significant improvement in intensities of RI beams, by more than three orders of magnitude. We could thus perform the first breakup experiments on ^{22}C and ^{31}Ne at RIBF. We measured breakup reactions both with Pb and C targets. Before this experiment, the heaviest $1n$ halo nucleus experimentally known had been ^{19}C . ^{22}C is the next $2n$ -halo candidate, since the two neutron separation energy S_{2n} is likely to be small and ^{21}C is unbound. The $2n$ separation energy of ^{22}C was estimated as 0.419 ± 0.935 MeV according to the mass evaluation in 2003 [13]. ^{31}Ne is the next heavier candidate for the $1n$ halo nucleus due to its small S_n . The mass evaluation [13] estimated $S_n = 0.332 \pm 1.069$ MeV, while the recent direct mass measurement extracted the value of 0.29 ± 1.64 MeV [14].

For ^{31}Ne , of particular interest is the fact that this nucleus is most likely in the island of inversion as the neighboring neon isotopes ^{30}Ne [15] and ^{32}Ne [16] are both in the island. The signal of halo itself is closely related to the shell melting since the halo formation means that the dominance configuration is not the $1f_{7/2}$ neutron on the $^{30}\text{Ne}(0_1^+)$ core which is expected for the nucleus with $N=21$ (magic number+1). Instead, the shell is modified such that the $2p_{3/2}$ orbit lowers below the $1f_{7/2}$ orbit, for instance.

4.1. Inclusive Coulomb breakup

Inclusive Coulomb breakup is useful for obtaining a signal of the existence of a halo structure. In an inclusive breakup experiment, we measure $1n(2n)$ removal cross section of a candidate nucleus with a heavy target. Namely, we measured the counts of $^{30}\text{Ne}(^{20}\text{C})$ fragments relative to the counts of $^{31}\text{Ne}(^{22}\text{C})$ projectiles which bombarded a Pb target in this experiment.

As mentioned, in an exclusive (kinematically complete) measurement four momentum vectors of all the outgoing particles are measured. Namely, a coincidence measurement of the neutron is necessary, which requires 1-2 order larger yield for the beam. On the other hand, an inclusive measurement is feasible with beam intensity of the order of counts per second or even less, suitable at the earlier stage of the new facility. Even at RIBF, inclusive measurements have

such advantage. In the experiment of Ref. [17], typical ^{31}Ne beam intensity was about 5 counts per second and the data was taken only for about 10 hours.

The inclusive Coulomb breakup works in the following way. The inclusive Coulomb breakup cross section $\sigma(E1)$ can be written as

$$\sigma(E1) = \int_{S_n}^{\infty} \frac{16\pi^3}{9\hbar c} N_{E1}(E_x) \frac{dB(E1)}{dE_x} dE_x. \quad (5)$$

Namely, the product of $N_{E1}(E_x)$ and $dB(E1)/dE_x$ is contained in the cross section.

As shown in Fig. 1, the photon spectrum falls exponentially with E_x . Thus, $\sigma(E1)$ becomes significant only when the $B(E1)$ is concentrated at low excitation energies as in the case of the soft $E1$ excitation. The bottom part of Fig.1 shows the comparison of calculations for an assumed halo nucleus (left;soft $E1$ excitation) and an assumed ordinary nucleus (right;GDR) for ^{31}Ne ($A=31$).

For the GDR, we assume that the ^{31}Ne is an ordinary typical nucleus with the GDR peak being located at the standard energy of $31.2 A^{-1/3} + 20.6 A^{-1/6}$ MeV=21.6 MeV with a width of 5 MeV. The amplitude is assumed to exhaust the full TRK sum rule. The TRK sum for the $A=31$ nucleus is 420 MeV-mb. The total Coulomb breakup cross section $\sigma(E1)$ in this case amounts to 58 mb.

On the other hand, assuming that ^{31}Ne is a halo nucleus and has large $E1$ strength at low energies caused by the valence neutron in $p_{3/2}$ with $S_n=0.5$ MeV, then the total Coulomb breakup cross section up to $E_x=10$ MeV is 510 mb, which is almost one order of magnitude larger than that of GDR. In the inclusive measurement, we obtain $1n$ removal Coulomb breakup cross section, whose integration ranges up to $E_x \sim S_{2n}$. For this range, almost no GDR strength can contribute to the Coulomb breakup, while the soft $E1$ excitation gives rise to the Coulomb breakup cross section of 470 mb. With such a distinctive difference, $1n$ -removal Coulomb breakup cross section can be used as a signal showing a halo state.

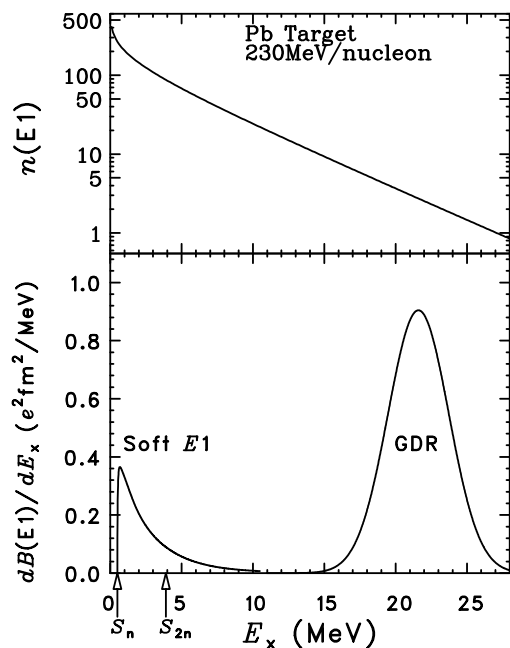


Figure 1. Top: $E1$ virtual photon spectrum for a Pb target at 230 MeV/nucleon. The impact parameter cut is assumed to be 13.1 fm. Bottom: The left peak is the calculation for the $B(E1)$ distribution assuming the soft $E1$ excitation of ^{31}Ne with the p -wave valence neutron bound by 0.5 MeV, while the right peak is the assumed GDR peak at $E_x=21.6$ MeV with the width of 5 MeV. The amplitude corresponds to the full TRK(Thomas Reich Kuhn) sum.

4.2. Results of inclusive Coulomb breakup of ^{31}Ne and ^{22}C

Figure 2 shows $1n$ removal cross sections for ^{19}C , ^{20}C , and ^{31}Ne , and $2n$ removal cross sections for ^{20}C and ^{22}C obtained for the Pb(dot-dashed line) and C(dotted line) targets at about 240 MeV/nucleon. The data for $^{20,22}\text{C}$ are preliminary and the detail will be published elsewhere. The detailed description of the ^{31}Ne breakup experiment is shown in Ref. [17]. The Coulomb breakup component of the $1n(2n)$ removal cross section on Pb was deduced by subtracting the nuclear component estimated from $\sigma_{-1n}(\text{C})$. Here, we assumed that $\sigma_{-1n}(\text{C})$ arises entirely from the nuclear contribution, and that the nuclear component for a Pb target scales with the parameter Γ , as in,

$$\sigma_{-1n}(E1) = \sigma_{-1n}(\text{Pb}) - \Gamma\sigma_{-1n}(\text{C}), \quad (6)$$

where Γ was estimated to be ~ 1.7 – 2.6 . The lower value is the ratio of target+projectile radii, while the upper one is that of radii of the two targets as in the Serber model [18]. We took into consideration the ambiguity arising from the choice of these two models.

Significant enhancement of the Coulomb breakup cross sections of $^{19}\text{C}(-1n)$, $^{22}\text{C}(-2n)$ and $^{31}\text{Ne}(-1n)$ is clearly shown. The cross sections are as large as the ones expected for those for the soft $E1$ excitation (0.5–1b). It should be noted that the ^{19}C is an established halo nucleus, and the Coulomb breakup cross section for ^{31}Ne is nearly as large as that for ^{19}C . The cross section for ^{22}C is even larger. With this comparison, we conclude that we have obtained evidence for the $1n$ halo structure in ^{31}Ne and $2n$ halo structure in ^{22}C .

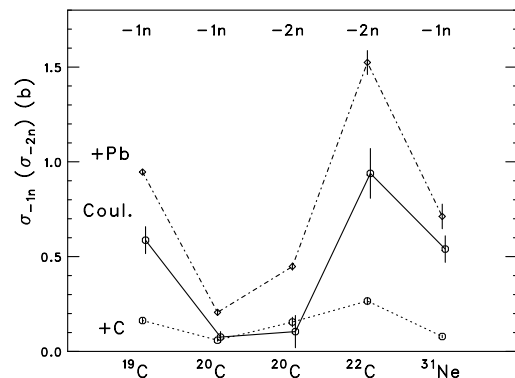


Figure 2. $1n$ removal cross sections for $^{19,20}\text{C}$ and ^{31}Ne , and $2n$ removal cross sections for $^{20,22}\text{C}$ with the Pb target(dot-dashed line) and the C target(dotted line). The extracted Coulomb breakup cross sections with the Pb target for these reaction channels are also shown (solid line).

4.3. Nuclear and Coulomb breakup with the associated γ -ray analysis

As discussed in Ref. [17], the halo structure of ^{31}Ne is either due to the $p_{3/2}$ or $s_{1/2}$ valence neutron. When we take into consideration the large scale Monte-Carlo shell model calculation [17], the p -wave halo case is more probable and the ground-state spin parity is $3/2^-$. As expected for the island-of-inversion nucleus, the ground state calculated is a mixture of several configurations. The major components are predicted to be $^{30}\text{Ne}(0_1^+) \otimes \nu 2p_{3/2}(C^2S = 0.12)$, $^{30}\text{Ne}(2_1^+) \otimes \nu 2p_{3/2}(C^2S = 0.27)$, and $^{30}\text{Ne}(2_1^+) \otimes \nu 1f_{7/2}(C^2S = 0.25)$. This implies that the $^{30}\text{Ne}(2_1^+)$ core components are significant.

In order to determine the detailed configuration, we have additionally measured γ rays associated with the daughter ^{30}Ne nucleus in the ^{31}Ne breakup with the C and Pb targets. A γ ray peak corresponding to the decay from the first excited state of ^{30}Ne at 792 keV was observed in the data of the C and Pb targets. The cross sections for $^{31}\text{Ne} \rightarrow ^{30}\text{Ne}(2_1^+)$ are 0.20(8) b for the Pb target, and 0.051(12) b for the C target (preliminary). This results in the estimation of the cross sections for $^{31}\text{Ne} \rightarrow ^{30}\text{Ne}(0_1^+)$ to be 0.52(1) b and 0.028(13) b, respectively. Since the direct transition to the ground state of ^{30}Ne is attributed to the $^{30}\text{Ne}(0_1^+) \otimes \nu 2p_{3/2}$ configuration only, we can estimate its C^2S as well as the S_n value of ^{31}Ne . The different dependence of

the cross sections on S_n between the Coulomb and nuclear breakup is used in the extraction of these values. The result is that $S_n=0.12(0.2)$ MeV, and $C^2S=0.28(0.23)$ for $^{30}\text{Ne}(0_1^+) \otimes \nu 2p_{3/2}$ (preliminary). Further analysis is under progress, including that of the momentum distribution of ^{30}Ne in the breakup with the carbon target, in order to further put the constraints on these key values.

5. Summary and future prospects

In this paper it has been shown that Coulomb and nuclear breakup experiments are very useful in investigating halo structures. The Coulomb breakup can probe the low-lying $E1$ strength (soft $E1$ excitation) which is a unique property of halo structures. By measuring all the momenta of outgoing particles in coincidence (exclusive measurement), one can determine the $B(E1)$ distribution, which can be related to the microscopic structure of halo nuclei. For the $1n$ halo nuclei, the shape and the amplitude of the spectrum can be understood in the framework of the direct breakup mechanism. There, the spectrum is strongly sensitive to S_n , ℓ of the valence neutron, and C^2S for the halo configuration, and hence these values can be extracted with such measurement. The s or p configuration is essential for the formation of halo due to none or very low centrifugal barrier. For two neutron halo nuclei dineutron correlation is probed additionally.

The nuclear breakup reaction, in particular one-neutron removal reaction, is a useful tool to determine the shell configuration, which involves the orbital angular momentum of the valence neutron and the core state with the associated C^2S value. The identification of the core final state is essential in this measurement. As an example of the unbound final core state, the experiment of $^{14}\text{Be} \rightarrow ^{13}\text{Be}$ was presented, where the intruder ^{13}Be ground state was identified for the first time.

The recent inclusive Coulomb breakup experiment of ^{22}C and ^{31}Ne at RIBF at RIKEN was then presented. The large Coulomb breakup cross section observed for ^{31}Ne and ^{22}C gave evidence of $1n$ halo structure in ^{31}Ne , and $2n$ halo structure in ^{22}C . For ^{31}Ne , a combined analysis of nuclear breakup and the γ ray analysis resulted in a preliminary conclusion that S_n of ^{31}Ne is as small as $0.12(0.2)$ MeV.

As demonstrated, the inclusive measurement is in particular important when the beam intensity is not sufficient. It provides us with the first approach to the exotic property of extremely neutron rich nuclei whose beam intensity is generally very weak. However, for the full understanding of the microscopic structure of ^{31}Ne , the exclusive Coulomb breakup experiment would be desired, where C^2S and S_n can be extracted directly.

At RIBF at RIKEN, such experiments will be realized by the completion of the SAMURAI (Superconducting Analyser for Multi-particles from Radio-Isotope Beam) facility, which is expected in 2012. The SAMURAI facility is equipped with a superconducting magnet with the 80 cm gap and the maximum magnetic field of about 3 T ($\sim 7\text{T}\cdot\text{m}$ bending power), and with the large-area neutron detectors, NEBULA (NEutron-detection system for Breakup of Unstable Nuclei with Large Acceptance). We plan to perform an exclusive Coulomb breakup experiment of ^{22}C and ^{31}Ne in the near future. Such an experiment would clarify further the microscopic structure (ℓ , shell configurations, S_n , S_{2n} etc.) of these exotic nuclei. There, experiments on the pygmy dipole resonance (PDR) for neutron-skin nuclei in heavier nuclei are also planned.

Acknowledgments

The Coulomb breakup experiment of ^{31}Ne and ^{22}C was performed in collaboration with N. Kobayashi, Y. Kondo, Y. Satou, N. Aoi, H. Baba, S. Deguchi, N. Fukuda, J. Gibelin, N. Inabe, M. Ishihara, D. Kameda, Y. Kawada, T. Kubo, K. Kusaka, A. Mengoni, T. Motobayashi, T. Ohnishi, M. Ohtake, N.A. Orr, H. Otsu, T. Otsuka, A. Saito, H. Sakurai, S. Shimoura, T. Sumikama, H. Takeda, E. Takeshita, M. Takechi, K. Tanaka, K.N. Tanaka, Y. Togano, Y. Utsuno, K. Yoneda, A. Yoshida, and K. Yoshida. The author would like to thank the

excellent delivery of the ^{48}Ca beam at RIKEN. The author acknowledges the support from the Nanoscience and Quantum Physics project of the Tokyo Institute of Technology through the Global Center of Excellence Program of the Ministry of Education, Culture, Sports, Science and Technology (MEXT), Japan. The present work was supported in part by a Grant-in-Aid for Scientific Research (B) (No. 22340053) from the Ministry of Education, Culture, Sports, Science and Technology (MEXT), Japan.

References

- [1] Sakurai H et al. 1999 *Phys. Lett. B* **448** 180.
- [2] Tanaka N et al. 2010 *Phys. Rev. Lett* **104** 062701.
- [3] Jensen A.S, Riisager K, and Fedorov D.V. 2004 *Rev. Mod. Phys.* **76**, 215.
- [4] Migdal A.B 1973 *Sov. J. Nucl. Phys.* **16** 238.
- [5] Hagino K 2007 *Phys. Rev. Lett.* **99** 022506.
- [6] Matsuo M 2006 *Phys. Rev. C* **73** 044309.
- [7] Nakamura T et al. 1994 *Phys. Lett. B* **331** 296.
- [8] Palit R. 2003 *Phys. Rev. C* **68** 034318.
- [9] Fukuda T et al. 2004 *Phys. Rev. C* **70** 054606.
- [10] Nakamura T et al. 1999 *Phys. Rev. Lett* **83** 1112.
- [11] Nakamura T et al. 2006 *Phys. Rev. Lett* **96** 252501.
- [12] Kondo Y et al. 2010 *Phys. Lett B* **690** 245.
- [13] Wapstra A.H., Audi G., and Thibault C. 2003 *Nucl. Phys. A* **729** 129; Audi G, Wapstra A.H., and Thibault C. 2003 *Nucl. Phys. A* **729** 337.
- [14] Jurado B et al. 2007 *Phys. Lett. B* **649** 43.
- [15] Yanagisawa Y et al. 2003 *Phys. Lett. B* **566** 84.
- [16] Doornenbal P et al. 2009 *Phys. Rev. Lett.* **103** 032501.
- [17] Nakamura T et al. 2009 *Phys. Rev. Lett.* **103** 262501.
- [18] Serber R 1947 *Phys. Rev.* **72** 1008.